JOURNAL OF VIROLOGY, Jan. 2005, p. 644–648 Vol. 79, No. 1
0022-538X/05/$08.00+0 doi:10.1128/JVI.79.1.644–648.2005

The Ubiquitin-Proteasome System Facilitates the Transfer of Murine Coronavirus from Endosome to Cytoplasm during Virus Entry

Guann-Yi Yu and Michael M. C. Lai*

Department of Molecular Microbiology and Immunology, Keck School of Medicine, University of Southern California, Los Angeles, California

Received 30 April 2004/Accepted 16 August 2004

The ubiquitin-proteasome system is involved in cellular endocytosis and maturation of some viruses. In this study, we found that proteasome inhibitors blocked mouse hepatitis virus replication at an early step in the viral life cycle. In the presence of MG132, the entering viruses accumulated in both the endosome and denser lysosome, suggesting that the ubiquitin-proteasome system is involved in the release of virus from the endosome to the cytosol during the virus entry step.

Mouse hepatitis virus (MHV) is an enveloped virus with a positive-stranded, nonsegmented RNA genome of about 32 kb (12). MHV belongs to the *Coronaviridae* family, which includes the recently emerged virus, severe acute respiratory syndrome (SARS) coronavirus (7). Since the ubiquitin-proteasome system is a fundamental machinery in the cell (9, 11, 14, 19) and has been shown to be involved in the replication, particularly virion maturation, of several viruses (4, 5, 8, 16–18), we are interested in knowing whether the ubiquitin-proteasome system is also involved in MHV replication.

The proteasome inhibitors blocked MHV (JHM strain) replication. To assess whether the proteasome-ubiquitin system plays a role in MHV (JHM strain) replication, irreversible (lactacystin) and reversible (MG132) proteasome inhibitors (13) were used to address the question. Neither of these two inhibitors affected cellular protein synthesis within the time frame of the experiment as determined by metabolic labeling with [^{35}S]methionine (data not shown). We also used the lactate dehydrogenase-based assay to test the cytotoxicity of these two proteasome inhibitors (Fig. 1A). The proteasome caused only slight cytotoxicity to DBT cells. When untreated cells were infected with MHV(JHM), the virus titer steadily increased logarithmically throughout the experiment; in contrast, in the presence of the proteasome inhibitors, either lactacystin or MG132, the virus production began approximately 8 h later than for the untreated cells, and the final virus titer at 24 h postinfection (p.i.) was 3 log units lower (Fig. 1B). Lactacystin and MG132 had very similar inhibitory effects on virus production. We also examined the kinetics of intracellular viral protein accumulation (Fig. 1C). The viral nucleocapsid N protein could be detected as early as 8 h p.i. in the untreated cells; in contrast, the N protein was not detected until 16 h p.i. (lactacystin) and 20 h p.i. (MG132), respectively. These data together indicated that proteasome inhibitors significantly blocked MHV production, suggesting that the proteasome may play an important role in MHV production.

* Corresponding author. Mailing address: Department of Molecular Microbiology and Immunology, Keck School of Medicine, University of Southern California, 2011 Zonal Ave., Los Angeles, CA 90033-1054. Phone: (323) 442-1748. Fax: (323) 442-1721. E-mail: michlai@hsc.usc.edu.

The proteasome-ubiquitin system is involved in an early step of virus replication. To elucidate the mechanism of inhibition, we took advantage of the reversible nature of MG132 to dissect the potential targets of the proteasome inhibitor. Figure 2A shows the experimental design for defining the major target of the ubiquitin-proteasome system by pulsing MG132 treatment (for 6 h) to MHV-infected cells at various time points in the viral life cycle. The medium was collected at the end of each 6-h period, and fresh medium was added. The harvested medium was used for plaque assays to determine the virus yield during the previous 6-h period. Figure 2B shows that no virus was produced from 0 to 6 h p.i. For virus that accumulated from 6 to 12 h p.i., the most dramatic inhibition by MG132 was seen with the treatment group in which MG132 was present throughout the experiment (pretreatment for 2 h plus treatment for the first 12 h p.i.). Treatment for 0 to 6 h also resulted in significant reduction of virus yield (2-log-unit reduction compared to the titer of the no-treatment control). The virus titer of the group treated for 6 to 12 h was 1 log unit lower than the titer of the control sample. For virus accumulated from 12 to 18 h p.i., the inhibitory effect was seen only in the group treated throughout. The virus titers from the 0- to 6-h, 6- to 12-h, and 12- to 18-h treatment groups were comparable to that of the no-treatment control during this time window, indicating that MG132 does not have significant effects on the later steps of the viral life cycle. The titer of virus that accumulated from 18 to 24 h p.i. was almost the same as that which accumulated from 6 to 12 h p.i. The 2-h pretreatment did not have any effect. The kinetic study results combined thus suggest that the proteasome-ubiquitin system is most likely involved at an early step in the virus life cycle, since the inhibitory effect of MG132 was seen primarily in the 0- to 6-h treatment group.

The proteasome inhibitor does not block virus internalization. Since the kinetic assay results showed that the proteasome-ubiquitin system likely works at an early step of viral replication, we dissected each step in the presence of the proteasome inhibitor to reveal the possible mechanism of inhibition. Both of the proteasome inhibitors did not affect the MHV receptor expression on the cell surface, as determined by surface staining with an MHV receptor-specific antibody and flow cytometry analysis (data not shown). Next, the virus internal-

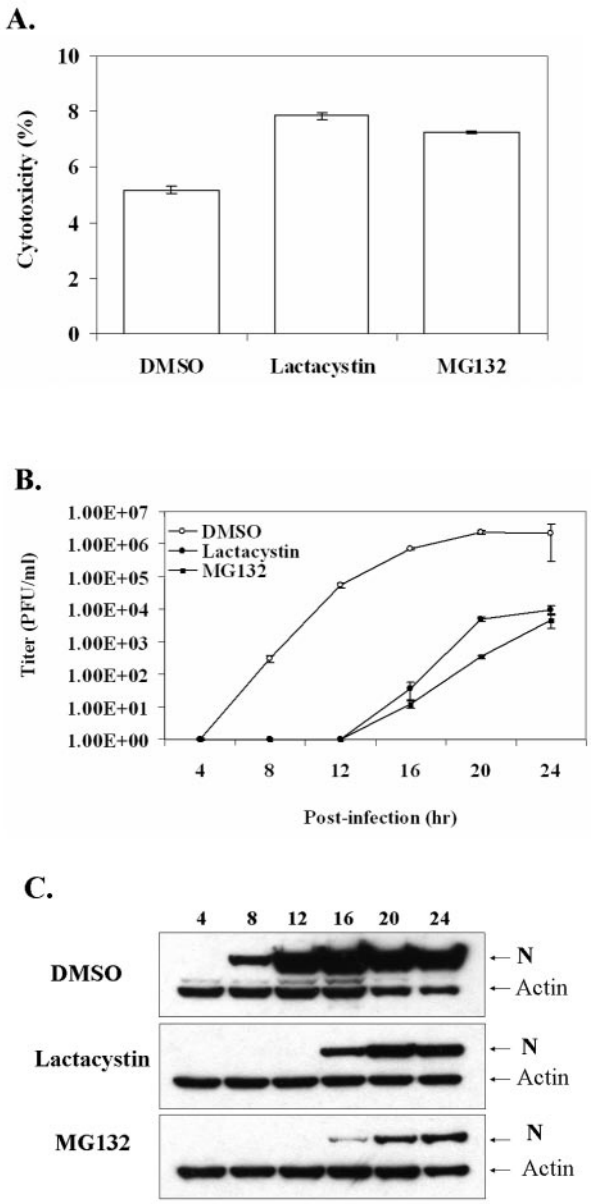

FIG. 1. The proteasome inhibitors lactacystin and MG132 blocked MHV(JHM) replication. (A) Cytotoxicity of lactacystin and MG132. DBT cells were treated with 5 μM lactacystin (Biomol, Plymouth, Pa.) or 5 μM MG132 (Biomol) or with the same volume of dimethyl sulfoxide (DMSO) (vehicle control) for 16 h and analyzed by CytoTox-One Homogeneous Membrane Integrity assay (Promega, Madison, Wis.). (B, C) Detection of virus production and viral protein synthesis for cells treated with a proteasome inhibitor. DBT cells, a mouse astrocytoma cell line (10), were pretreated with lactacystin (5 μM), MG132 (5 μM), or DMSO for 2 h, infected with MHV(JHM) (multiplicity of infection of 0.1) for 1 h, and then incubated at 37°C for different lengths of time in the presence or absence of the proteasome inhibitors. (B) Virus titers in the culture medium were determined by plaque assay (1). Standard variations were calculated from three replicate samples of each treatment. 1.00E+00, 1×10^0. (C) The infected cells were also collected for detection of viral N protein by Western blotting using monoclonal antibody J3.3 (3). β-Actin was used as an internal control.

ization assay was performed (1) (Fig. 3A). After 2-h pretreatment with MG132, the cells were incubated with MHV at 4°C for 1 h to allow virus binding and then incubated at 37°C for an additional hour to allow virus internalization. Afterwards, the cells were treated with proteinase K to remove the virus remaining on the cell surface. The cells were then serially diluted and mixed with uninfected cells for infectious center assay. Once the virus is internalized in a cell, it is expected to yield a plaque in this assay (1, 15). Since MHV(JHM) enters cells by both endosomal and nonendosomal pathways (14, 18) and endocytosis is an energy-dependent process, very little virus was internalized at 4°C; therefore, most of the virus was digested away by proteinase K (Fig. 3A). In contrast, at 37°C, a significantly higher titer of virus was internalized in the cell and was protected from proteinase K digestion. There was no difference in infectious center titer in the presence or absence of the proteasome inhibitor. These data suggest that the proteasome-ubiquitin system is not involved in the virus internalization step.

Next, we monitored the fate of the internalized virus particles in the endosomes. Endosomes from the infected cells were purified by use of a sucrose flotation gradient (6), and the viruses were traced by reverse transcription-PCR (RT-PCR) of viral RNA (Fig. 3B, left gel). After centrifugation, the late endosomes floated to the interface between 8 and 25% sucrose (fractions 1 to 3), and the early endosomes floated to the interface between 25 and 35% sucrose (fractions 4 to 7, the early endosome marker in Fig. 3C). Fractions 8 to 10 contained the cytosol and other organelles (the cytosol and endoplasmic reticulum [ER] markers in Fig. 3C). Significantly more viral RNAs were detected in the early and late endosome fractions in the presence of MG132 compared to the control samples (Fig. 3B, left gel). Only in the presence of MG132 was the viral RNA detected in fractions 1 to 3, the reported late endosome fractions (6). Figure 3B, right gel, shows the total viral RNA in the lysate used for sucrose gradient sedimentation. There was more viral RNA from the untreated cells than from the MG132-treated cells, consistent with the interpretation that MG132 blocked virus entry and subsequent viral replication. These results show that the virus is retained in the endosomes in the absence of a functional ubiquitin-proteasome system.

The proteasome inhibitor directs viruses to the lysosomes. This result prompted us to purify lysosomes to determine whether the virus is misdirected to the lysosomes when the ubiquitin-proteasome system is not functioning. Ultracentrifuge sedimentation of cellular lysates on a 27% Percoll gradient was performed to partially purify lysosomes (2) (Fig. 4). The activity of the lysosomal resident enzyme, acid phosphatase, was detected in fractions 1 and 2 as well as fractions 9 to 11 (Fig. 4B). Most of the other organelles were localized in fractions 9 to 11 (Fig. 4B, ER marker and cytosol marker). In the control cells, viruses were detected only in fraction 9 (Fig. 4A). In contrast, viruses were detected mostly in fractions 2 to 6 in the MG132-treated cells. Fractions 10 and 11 in both treated and untreated cells also contained a large amount of nonspecific RNA but no distinct viral RNA. We subsequently found that viral RNA was also present in fractions 10 and 11 in both the treated and untreated cells; however, the presence of a large amount of cellular RNA in these two fractions interfered with the detection of viral RNA by RT-PCR. When the

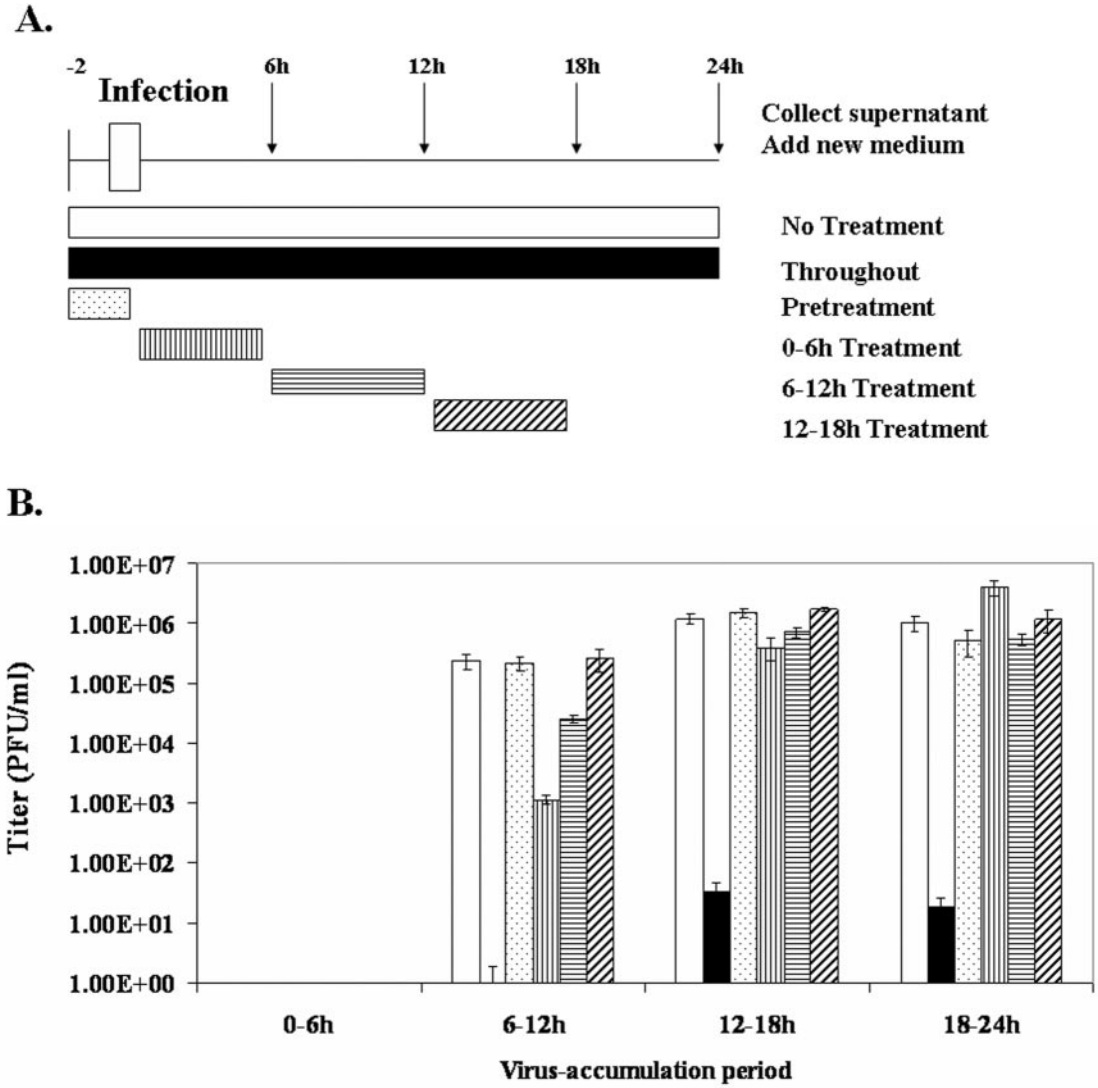

FIG. 2. Kinetics of virus replication after pulse treatment with MG132. (A) Experimental design for pulse treatment with MG132. The cells were treated with MG132 during different time windows. Culture medium was collected, and fresh medium was replenished at 6-h intervals. (B) The virus titer at each time point was detected by a plaque assay. Standard variations were calculated from three replicate samples of each treatment. 1.00E+00, 1×10^0.

RNA samples were diluted 100-fold, viral RNA was detected in these two fractions in both the control cells and MG132-treated cells (Fig. 4C). Significantly more viral RNA was present in these two fractions in the control cells than in the MG132-treated cells.

To investigate the nature of the viral RNAs in each fraction, each fraction was treated with RNase A and then subjected to RT-PCR treatment. All of the viral RNAs in fractions 1 through 9 from the MG132-treated cells were resistant to RNase A (data not shown). In contrast, viral RNAs in fractions 10 and 11 from the control cells were sensitive to RNase A, suggesting that they were released from the organelles (Fig. 4C). By comparison, most of the viral RNA in fractions 10 and 11 from the MG132-treated cells was resistant to RNase A (Fig. 4C), consistent with the interpretation that viruses remained enclosed within vesicles. We concluded that, in the presence of MG132, most virus remained in vesicles, either endosomes or lysosomes, and thus, are protected from RNase digestion. Therefore, even though MHV can be internalized in the cell in the absence of a functional ubiquitin-proteasome system, the viruses within endosomes or lysosomes cannot be released into the cytosol.

We attempted to demonstrate whether any of the viral proteins were ubiquitinated. None of the viral structural proteins could be detected by immunoprecipitation with antiubiquitin antibody; nor could we detect any ubiquitinated cellular proteins specifically associated with the MHV virion in the endosome (namely, no ubiquitinated host factor was pulled down specifically by MHV antiserum after chemical cross-linking in the presence of a proteasome inhibitor). We also found that the MHV receptor is not ubiquitinated and that overexpression of an MHV receptor-ubiquitin fusion protein could not rescue viruses from MG132-induced inhibition. Therefore, precisely how the ubiquitination-proteasome system helps to

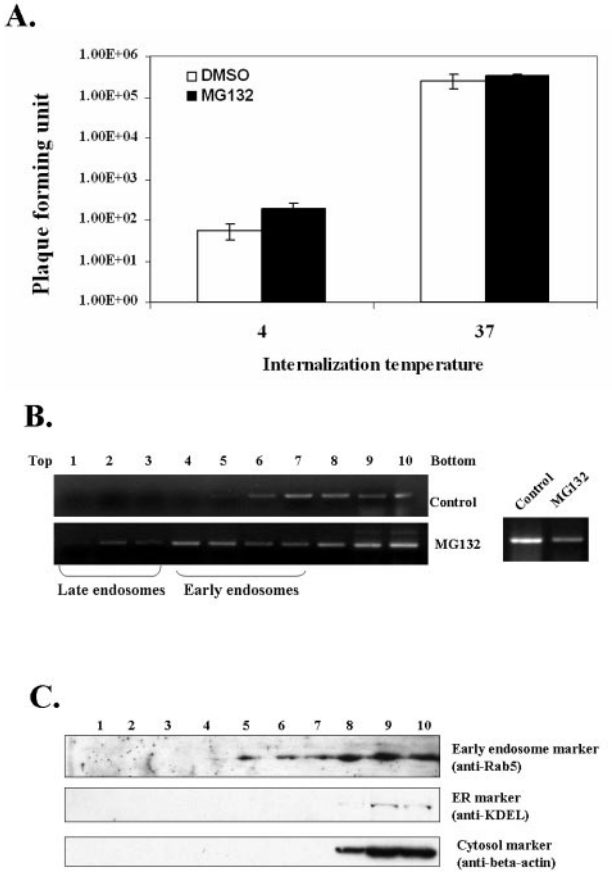

FIG. 3. (A) Effect of MG132 on virus internalization. Virus internalization assay was performed as described previously (1). DBT cells preincubated for 2 h with or without MG132 were incubated with MHV(JHM) at 4°C for 1 h (multiplicity of infection [MOI] of 0.1). After cells were washed with medium, they were either maintained at 4°C or shifted to 37°C for one more hour for virus internalization. Afterwards, infected cells were treated with proteinase K (50 μg/ml) to remove noninternalized viruses. The treated cells were diluted in serial 10-fold dilutions with untreated DBT cells and plated onto a six-well plate. Five hours later, the medium was removed, and the plates were overlaid with agar as in the plaque assay. After 48-h incubation, plaques were counted after neutral red staining. (B) Endosome purification by flotation gradient. DBT cells were treated with MG132 for 2 h, infected with MHV(JHM) for 1 h (MOI of 0.1), and incubated at 37°C for three more hours in the presence or absence of MG132. The infected cells were collected and examined by a sucrose flotation assay (6). Cells were lysed in 0.5 ml of homogenization buffer (250 mM sucrose, 1 mM EDTA, 1 mM phenylmethylsulfonyl fluoride [PMSF]) by passage through a 22-gauge needle 10 times. The supernatant (postnuclear supernatant [PNS]) was collected after centrifugation (1,000 × *g*) and was adjusted to a concentration of 40.6% sucrose and 1 mM EDTA. One milliliter of PNS in 40.6% sucrose was transferred to the bottom of an SW55Ti tube and overlaid sequentially with 2 ml of 35% sucrose, 1.5 ml of 25% sucrose, and 1 ml of homogenization buffer. After centrifugation (100,000 × *g*, 4°C, 1 h), samples were collected from the top to the bottom in 1-ml fractions. The fraction numbers are shown above the gel. Total RNA was extracted from each fraction by using TRI REAGENT-LS (Molecular Research Center, Cincinnati, Ohio), and viral RNA was detected by RT-PCR using primers 5′TA TAAACGGCACTTCCTGCG3′ (forward) and 5′AACCCATCCTCC TCTGACCT3′ (reverse) [the 5′ untranslated region of MHV(JHM) RNA]. An aliquot of PNS before sucrose gradient sedimentation was used to quantitate the total amount of viral RNA in the treated and untreated cells (right gel). (C) Various organelle markers, including Rab5 (early endosome marker; Stressgen Biotechnologies Corporation, Victoria, British Columbia, Canada), Grp78 (ER marker, anti-KDEL antibody; Stressgen), and β-actin (cytosol marker) were detected by Western blotting.

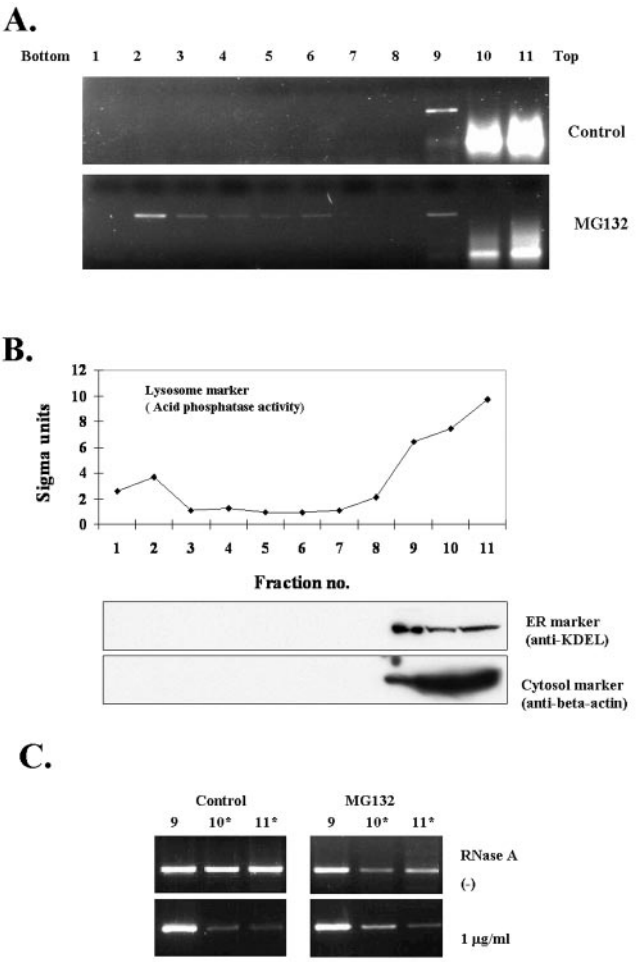

FIG. 4. Detection of viruses in the dense lysosome fractions. DBT cells were treated with or without MG132 as described in the legend to Fig. 3 and harvested for Percoll gradient centrifugation (2). Cells were lysed in 2 ml of homogenization buffer (250 mM sucrose, 1 mM EDTA, 1 mM PMSF) by passage through a 22-gauge needle seven times. After centrifugation at 1,000 × *g* for 10 min, the postnuclear supernatant was collected and put on top of a 27% Percoll gradient (1-ml cushion of 2.5 M sucrose at the bottom and 9 ml of 27% Percoll solution in 250 mM sucrose–1 mM EDTA), and the gradient was spun at 34,000 × *g* (SW41) at 4°C for 1 h. Samples were collected at 1 ml/fraction from the bottom to the top. The fraction numbers are shown above the gel. (A) Viral RNA of each fraction was detected by RT-PCR. (B) Acid phosphatase activity analyzed by using an acid phosphatase kit (Sigma, Saint Louis, Mo.). Acid phosphatase activity served as a lysosome marker. Other organelle markers (Grp78 and β-actin) were detected by Western blotting. (C) RNase sensitivity assay. Fractionated samples (fractions 9, 10, and 11) from Percoll gradient were treated with RNase A (1 μg/ml) or not treated with RNase A, and viral RNA was detected by RT-PCR of the 5′ untranslated region. RNA samples from fractions 10 and 11 that were diluted 100-fold for the RT reaction are indicated by asterisks.

release the virion from the endosome is still unclear. MHV has been shown to enter cells through both membrane fusion and endocytosis processes, depending on virus strain and cell type (15). It is likely that only the endocytic process requires the

ubiquitin-proteasome system (19). Indeed, we found that another MHV strain (A59) was less sensitive to the ubiquitin-proteasome inhibitors (unpublished observation). Correspondingly, MHV(A59) enters cells by an energy-independent, presumably membrane fusion, mechanism (unpublished observation). Thus, sensitivity to the ubiquitin-proteasome inhibitors may be used to distinguish the mechanism of viral entry. Understanding the mechanism of ubiquitin involvement in MHV entry will thus contribute to our understanding of the early steps of viral replication.

This work was partially supported by National Institutes of Health research grant AI19244.

REFERENCES

1. **Asanaka, M., and M. M. C. Lai.** 1993. Cell fusion studies identified multiple cellular factors involved in mouse hepatitis virus entry. Virology **197:**732–741.
2. **Driessen, C., R. A. Bryant, A. M. Lennon-Dumenil, J. A. Villadangos, P. W. Bryant, G. P. Shi, H. A. Chapman, and H. L. Ploegh.** 1999. Cathepsin S controls the trafficking and maturation of MHC class II molecules in dendritic cells. J. Cell Biol. **147:**775–790.
3. **Fleming, J. O., S. A. Stohlman, R. C. Harmon, M. M C. Lai, J. A. Frelinger, and L. P. Weiner.** 1983. Antigenic relationships of murine coronaviruses: analysis using monoclonal antibodies to JHM (MHV-4) virus. Virology **131:** 296–307.
4. **Galinier, R., E. Gout, H. Lortat-Jacob, J. Wood, and J. Chroboczek.** 2002. Adenovirus protein involved in virus internalization recruits ubiquitin-protein ligases. Biochemistry **41:**14299–14305.
5. **Gao, L., H. Tu, S. T. Shi, K. J. Lee, M. Asanaka, S. B. Hwang, and M. M. C. Lai.** 2003. Interaction with a ubiquitin-like protein enhances the ubiquitination and degradation of hepatitis C virus RNA-dependent RNA polymerase. J. Virol. **77:**4149–4159.
6. **Gruenberg, J., and J.-P. Gorvel.** 1997. In vitro reconstitution of endocytic vesicle fusion, p. 186. *In* J. M. Graham and D. Rickwood (ed.), Subcellular fractionation: a practical approach. IRL Press, New York, N.Y.
7. **Guan, Y., B. J. Zheng, Y. Q. He, X. L. Liu, Z. X. Zhuang, C. L. Cheung, S. W. Luo, P. H. Li, L. J. Zhang, Y. J. Guan, K. M. Butt, K. L. Wong, K. W. Chan, W. Lim, K. F. Shortridge, K. Y. Yuen, J. S. Peiris, and L. L. Poon.** 2003. Isolation and characterization of viruses related to the SARS coronavirus from animals in southern China. Science **302:**276–278.
8. **Harty, R. N., M. E. Brown, J. P. McGettigan, G. Wang, H. R. Jayakar, J. M. Huibregtse, M. A. Whitt, and M. J. Schnell.** 2001. Rhabdoviruses and the cellular ubiquitin-proteasome system: a budding interaction. J. Virol. **75:** 10623–10629.
9. **Hicke, L.** 2001. A new ticket for entry into budding vesicles—ubiquitin. Cell **106:**527–530.
10. **Hirano, N., K. Fujiwara, S. Hino, and M. Matumoto.** 1974. Replication and plaque formation of mouse hepatitis virus (MHV-2) in mouse cell line DBT culture. Arch. Gesamte Virusforsch. **44:**298–302.
11. **Hoege, C., B. Pfander, G. L. Moldovan, G. Pyrowolakis, and S. Jentsch.** 2002. RAD6-dependent DNA repair is linked to modification of PCNA by ubiquitin and SUMO. Nature **419:**135–141.
12. **Lai, M. M. C., and D. Cavanagh.** 1997. The molecular biology of coronaviruses. Adv. Virus Res. **48:**1–100.
13. **Lee, D. H., and A. L. Goldberg.** 1998. Proteasome inhibitors: valuable new tools for cell biologists. Trends Cell Biol. **8:**397–403.
14. **Muratani, M., and W. P. Tansey.** 2003. How the ubiquitin-proteasome system controls transcription. Nat. Rev. Mol. Cell Biol. **4:**192–201.
15. **Nash, T. C., and M. J. Buchmeier.** 1997. Entry of mouse hepatitis virus into cells by endosomal and nonendosomal pathways. Virology **233:**1–8.
16. **Reichel, C., and R. N. Beachy.** 2000. Degradation of tobacco mosaic virus movement protein by the 26S proteasome. J. Virol. **74:**3330–3337.
17. **Ros, C., C. J. Burckhardt, and C. Kempf.** 2002. Cytoplasmic trafficking of minute virus of mice: low-pH requirement, routing to late endosomes, and proteasome interaction. J. Virol. **76:**12634–12645.
18. **Schubert, U., D. E. Ott, E. N. Chertova, R. Welker, U. Tessmer, M. F. Princiotta, J. R. Bennink, H. G. Krausslich, and J. W. Yewdell.** 2000. Proteasome inhibition interferes with gag polyprotein processing, release, and maturation of HIV-1 and HIV-2. Proc. Natl. Acad. Sci. USA **97:**13057–13062.
19. **Strous, G. J., and R. Govers.** 1999. The ubiquitin-proteasome system and endocytosis. J. Cell Sci. **112:**1417–1423.